

# Hydrogen-Bonded Helical Hydrazide Oligomers and Polymer That Mimic the Ion Transport of Gramicidin A

Pengyang Xin, Pingping Zhu, Pei Su, Jun-Li Hou,\* and Zhan-Ting Li\*

Department of Chemistry, Fudan University, 220 Handan Road, Shanghai 200433, China

**S** Supporting Information

**ABSTRACT:** A new series of hydrogen-bonded helical aromatic hydrazide oligomers and polymer that bear phenylalanine tripeptide chains have been designed and synthesized. It was revealed that the helical structures could insert into lipid bilayers to form unimolecular channels. The longest oligomeric and polymeric helical channels exhibited an  $\text{NH}_4^+/\text{K}^+$  selectivity that was higher than that of natural gramicidin A, whereas the transport of a short helical channel for  $\text{Tl}^+$  could achieve an efficiency as high as that of gramicidin A.

Natural ion channels are proteins that form porous structures in lipid bilayers to mediate the transport of ions.<sup>1</sup> One of the best-characterized channels is gramicidin A (gA), a linear pentadecapeptide that consists of D- and L-amino acids. The two different kinds of amino acids are arranged alternately in the backbone, resulting in a well-defined porous  $\beta$ -helix for selective transmembrane transport of cations.<sup>2</sup> Because of its structural simplicity, gA has been considered as the most important natural prototype for the design of artificial systems.<sup>3</sup> In the last three decades, considerable effort has been devoted to the construction of artificial ion channels on the basis of the supramolecular strategy.<sup>4–7</sup> Several single-molecular mimicking systems have also been reported.<sup>8–12</sup> In spite of the important advances, the design of artificial structures with selectivity and efficiency comparable to those of natural channels has been a challenge. One of the most important factors that control the selectivity and efficiency of transport is the stability of the required conformation of the molecular and supramolecular systems.<sup>1</sup> Given the conformational preorganization of hydrogen-bonded aromatic amide- and hydrazide-based foldamers,<sup>13</sup> we have designed and prepared a series of hydrazide oligomers and polymers. Herein we demonstrate that their folded and helical conformation exhibited cation transport selectivity and efficiency that are comparable to or higher than those of gA.

We had established that intramolecular hydrogen bonding induces linear oligohydrazides to form helical conformations that generate a well-defined cavity with a diameter of 1.0 nm.<sup>14</sup> We recently found that phenylalanine (Phe) tripeptide was able to enhance the insertion of aromatic frameworks into lipid bilayers.<sup>15</sup> We thus prepared oligomers 1–4 and polymer 5 (Figure 1). The molecular weight of polymer 5 was determined to be 15810 by gel-permeation chromatography using the standard curve method [Figures S43 and S44 in the Supporting Information (SI)],<sup>16</sup> which corresponded to a polymerization degree of about 10. Molecular modeling of 2–5 showed that they

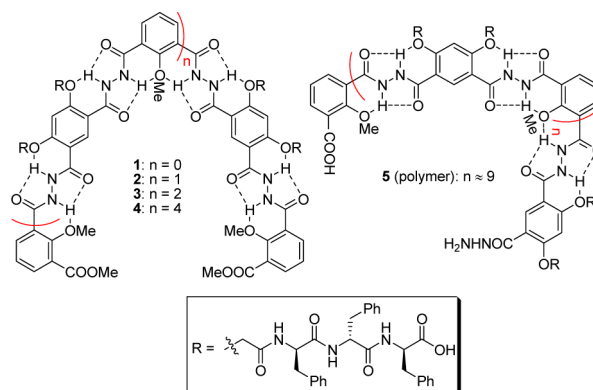


**Figure 1.** Structures of oligomers 1–4 and polymer 5.

exhibited 0.9, 1, 2, and 3.5 helix turns, respectively. Although the oligomers and polymer contain chiral side chains, circular dichroism experiments indicated that they did not induce the aromatic hydrazide backbone to produce helicity bias (see section S7 in the SI).

The possibility of incorporating 1–5 into lipid bilayers, whose concentration could be determined accurately, was first tested by assessing their proton transport activity on vesicles.<sup>17</sup> A suspension of vesicles (pH 7.2 inside the vesicle) composed of egg yolk L- $\alpha$ -phosphatidylcholine (EYPC) entrapping the pH-sensitive dye 8-hydroxypyrene-1,3,6-trisulfonate (HPTS) (0.1 mM) was prepared and then added to a buffer (pH 6.0) to produce a higher  $\text{H}^+$  concentration outside the vesicles. The flux of  $\text{H}^+$  into the vesicles mediated by 1–5 was assessed by monitoring the fluorescence intensity of HPTS. With the addition of 0.2% 1–5 (molar ratio relative to lipid, represented by  $x$ ),<sup>18</sup> the fluorescence intensity of HPTS increased significantly and reached 37%, 40%, 48%, 58%, and 79%, respectively, after 8 min (Figure 2a). These results demonstrated that all of the compounds were able to insert into bilayers and transport  $\text{H}^+$ . Further fluorescence experiments in the presence of valinomycin, a selective  $\text{K}^+$  carrier, indicated that  $\text{H}^+/\text{Cl}^-$  symport balanced the charges (see section S4). The  $\text{H}^+$  transport by 1–5 at different  $x$  was also investigated (Figure S45). The effective concentration needed for 50% activity ( $\text{EC}_{50}$ ) was calculated by fitting the plot of the relative fluorescence intensity at  $t = 8$  min versus  $x$  with the Hill equation.<sup>19</sup> The results are shown in Figure 2b. It was found that the  $\text{EC}_{50}$  value decreased in the order  $1 > 2 > 3 > 4 \gg 5$ , indicating that the transport activity

Received: April 4, 2014

Published: September 4, 2014

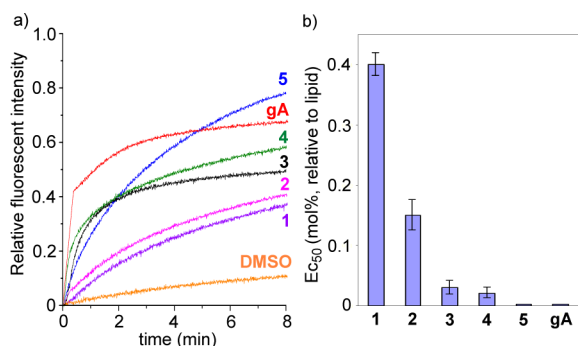


**Figure 2.** (a) Changes in fluorescence intensity of HPTS ( $\lambda_{\text{ex}} = 460$  nm,  $\lambda_{\text{em}} = 510$  nm) in vesicles with time after addition of 1–5 and gA ( $x = 0.2\%$ ). (b) Effective concentration needed for 50% activity ( $EC_{50}$ ) of 1–5 and gA.

increased with elongation of the backbone. Polymer 5 displayed the highest activity with an  $EC_{50}$  as low as 0.003%, which is close to that of gA ( $EC_{50} = 0.002\%$ ).

It has been established that transmembrane transport can be achieved via carrier,<sup>20</sup> relay,<sup>21</sup> or channel mechanisms.<sup>22</sup> To investigate the transport mechanism of 1–5, patch clamp experiments on a planar lipid bilayer were performed.<sup>23</sup> For these experiments, two compartments containing  $\text{NH}_4\text{Cl}$  solution (1.0 M) were separated by a planar lipid bilayer composed of diphytanoylphosphatidylcholine (diPhyPC). The solution of 1–5 in DMSO was added to the cis compartment, which was grounded. A clamped voltage of +100 mV was applied across the bilayer, and the conductance traces were recorded (Figure 3).

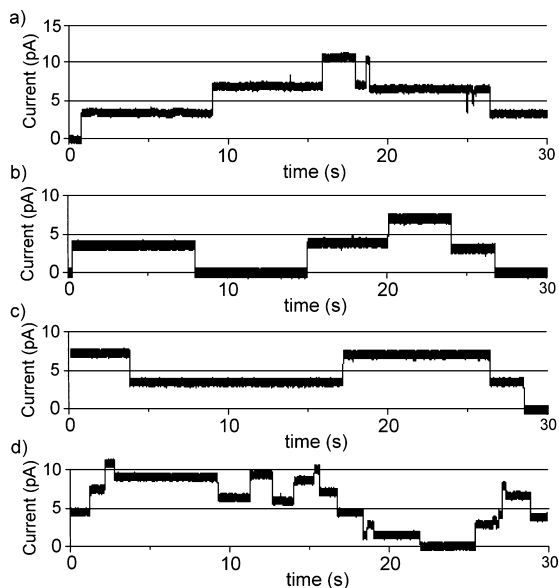


**Figure 3.** Current traces (30 s) of (a) 2, (b) 3, (c) 4, and (d) 5 ( $0.5 \mu\text{M}$ ) in the planar lipid bilayer at +100 mV in a symmetrical  $\text{NH}_4\text{Cl}$  solution (1.0 M).

Upon addition of oligomers 2–4 ( $0.5 \mu\text{M}$ ), the conductance traces displayed very regular squarelike signals, strongly supporting the formation of transmembrane  $\text{NH}_4^+$  channels in the lipid bilayer (Figure 5, *vide infra*). Although the traces showed multiple levels of currents, the current at each level was identical. This result clearly indicated that they had only one conductance state, which implied that only the folded or helical

conformation existed in the bilayer. The lifetimes of the open channels were in the range of 0.5–10 s, suggesting that the active channel conformations were quite stable in the bilayer.<sup>24</sup> Under the same conditions, the addition of 1 did not generate any conductance signals. This observation suggested that this rodlike compound could not form channels in the lipid bilayer and that the above weak  $\text{H}^+$  transport by it (Figure 2a) might occur via the carrier mechanism. Polymer 5 ( $0.5 \mu\text{M}$ ) could also form channels of long open duration (Figure 3d). However, different from 2–4, this polymeric sample generated a trace of multiple currents, which can be attributed to the different length of the polymeric components.

Patch clamp experiments for 2–5 at different voltages were also performed (Figure 4). All of the samples displayed a linear

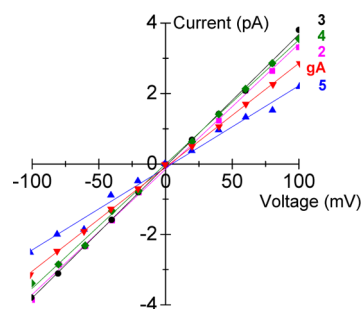


**Figure 4.**  $I-V$  plots for 2–5 and gA ( $0.5 \mu\text{M}$ ) in the planar lipid bilayer in a symmetrical  $\text{NH}_4\text{Cl}$  solution (1.0 M).

current–voltage ( $I-V$ ) relationship in the range of  $-100$  to  $+100$  mV. Their corresponding conductances ( $\gamma$ ) for  $\text{NH}_4^+$  were calculated to be  $35.5 \pm 0.5$ ,  $37.2 \pm 0.4$ ,  $35.0 \pm 0.5$ , and  $24.2 \pm 0.7$  pS, respectively.<sup>25</sup> It had been reported that gA has a high transport activity toward  $\text{NH}_4^+$ .<sup>26</sup> For comparison, the transport of gA for  $\text{NH}_4^+$  was also monitored under the present measurement conditions, and  $\gamma$  was determined to be  $32 \pm 0.6$  pS. The  $\gamma$  values of 2–4 were even higher than that of gA, demonstrating that the  $\text{NH}_4^+$  transport efficiencies of these helical structures were higher than that of gA. Similar patch clamp experiments were also performed for the chloride salts of  $\text{Na}^+$ ,  $\text{K}^+$ ,  $\text{Rb}^+$ , and  $\text{Cs}^+$  (see the SI), which revealed that the four helical samples could transport all of these cations. Their  $\gamma$  values for these ions were close to the corresponding values of gA for the same ions.

The transport selectivities of 2–5 for the above five cations and chloride anion were measured by using unsymmetrical salt solutions on the two sides of the bilayer. From the corresponding  $I-V$  curves, we could determine their reversal potentials ( $\epsilon_{\text{rev}}$ ) for the respective ions (Figures S45–S50) and the permeability ( $P$ ) ratios using the Goldman–Hodgkin–Katz equation (Figure 5).<sup>27</sup> All of the channels displayed transport selectivity for alkaline cations over chloride anion and, for the alkaline cations, the selectivity was in the order of  $\text{Cs}^+ > \text{Rb}^+ > \text{K}^+ > \text{Na}^+$ . This sequence is consistent with the Eisenman I sequence caused by dehydration of the cations.<sup>28,29</sup>  $^1\text{H}$  NMR experiments in  $\text{CDCl}_3$  for esters 10, 13, 15, 17, and 18 (Scheme S1 in the SI) showed that they did not bind the above cations (see section S8), which also implies that the above selectivity sequence was caused by the increased dehydration penalty of the cations. Similar to gA, 2–5 also displayed the highest  $\text{NH}_4^+/\text{K}^+$  selectivities, which can be rationalized by considering that in addition to electrostatic interactions,  $\text{NH}_4^+$  can form intermolecular hydrogen bonds with the carbonyl oxygens located in the cavity of the helical

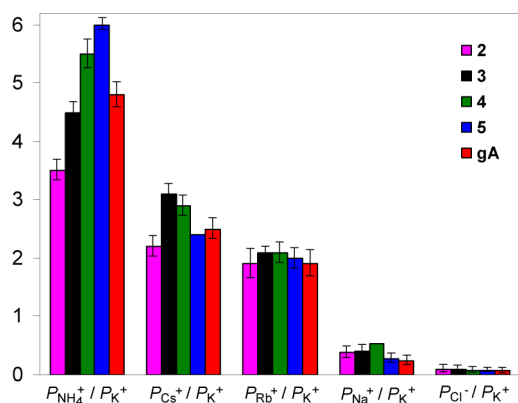


**Figure 5.** Permeability ( $P$ ) ratios of ions through the channels formed by 2–5 and gA, revealing the selectivity of the helical channels.

backbones.<sup>30,31</sup> The fact that the  $\text{NH}_4^+/\text{K}^+$  selectivity increased considerably with the elongation of the helical backbone also supports the mediation of this intermolecular hydrogen bonding in promoting the transport of  $\text{NH}_4^+$ .

To measure the kinetics of the transport process, stopped-flow experiments were carried out for 1–5 and gA for comparison.<sup>32</sup> Because it is difficult to measure the transport kinetics of the above ions, we chose to measure the rate of  $\text{Tl}^+$  flux into vesicles by recording its quenching of the fluorescence of 8-aminonaphthalene-1,3,6-trisulfonic acid disodium salt (Ants).<sup>31</sup>  $\text{Tl}^+$  has a radius very close to that of  $\text{K}^+$ ,<sup>33</sup> and it has been used as an analogue of  $\text{K}^+$  to study the transport mechanism of colicin E1.<sup>32b</sup> Vesicles containing Ants (20 mM) were prepared and incubated with 1–5 (2.5  $\mu\text{M}$ ). The flux of  $\text{Tl}^+$  was initiated by quickly mixing the vesicle solution with the same volume of  $\text{TlNO}_3$  solution (50 mM) in the stopped-flow spectrophotometer, and the fluorescence intensity of Ants was monitored (Figure 6a).

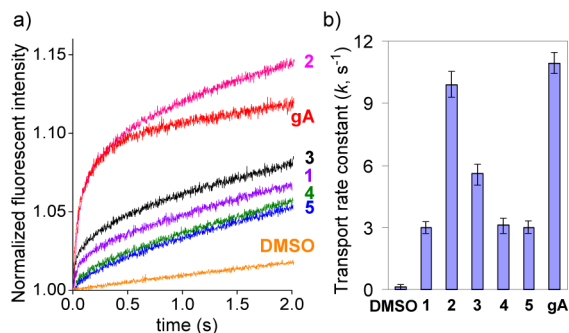


**Figure 6.** Normalized stopped-flow fluorescence intensity of Ants ( $\lambda_{\text{ex}} = 370$  nm,  $\lambda_{\text{em}} = 515$  nm). Vesicles loaded with Ants (20 mM) were incubated with DMSO, 1–5, or gA (2.5  $\mu\text{M}$ ). At  $t = 0$  s, the vesicle solutions were quickly mixed (dead time = 0.2 ms) with buffer containing  $\text{TlNO}_3$  (50 mM).

Compared with the control, the presence of 1–5 and gA promoted the quenching of the fluorescence of Ants by  $\text{Tl}^+$ . By fitting the curves to the first-order kinetic equation, we determined the rate constants ( $k$ ) for the transport of  $\text{Tl}^+$  by 1–5 (Figure 6b). Although the values for the systems of 3–5 were relatively low, the value for 2 was quite close to that of gA. A comparison of the values for 2–5 revealed that the transport rate decreased with the length of the helical backbone. This result implies that the passage of  $\text{Tl}^+$  through the cavity of the helical backbone is rate-determining and thus that the short backbones

allow  $\text{Tl}^+$  to pass more quickly because the ion suffers decreased electrostatic “dragging”. The  $k$  value of the shortest trimer 1 was the lowest, indicating that it mediated the transport of  $\text{Tl}^+$  also in the carrier mechanism.

Stopped-flow experiments for the transport of  $\text{Tl}^+$  have also been demonstrated to be a reliable technique for the determination of the molecularity of natural ion channels.<sup>32b</sup> We conducted similar experiments at different concentrations of 2–5 to establish their molecularity. To do this, the initial transport rates ( $V_0$ ) for the transport of  $\text{Tl}^+$  by the channels were calculated from the slopes of the curves at  $t = 0$  s. In the absence of the helical species, the diffusion rate of  $\text{Tl}^+$  across bilayers was much lower (by 52-fold), and thus, in the presence of the helical channels, the diffusion-caused flux of  $\text{Tl}^+$  was negligible. For 2 and 3, the  $\log V_0$  values were found to have a linear relationship with  $\log [2]$  or  $\log [3]$  (Figure 7a), and their slopes ( $n$ ) were

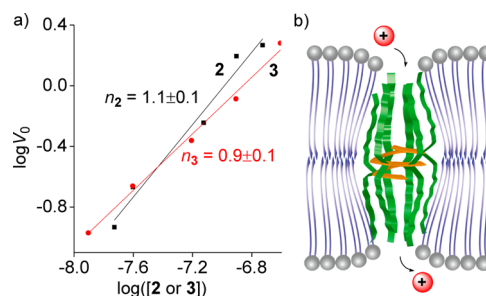


**Figure 7.** (a) Plots of  $\log V_0$  vs  $\log [2]$  and  $\log [3]$ . (b) Schematic presentation of the transmembrane channel formed by the helical structures.

determined to be  $1.1 \pm 0.1$  and  $0.9 \pm 0.1$ , respectively. Further UV dilution experiments of two helical ester analogues in chloroform (Figure S54) showed that no exergonic self-assembly took place from 50 to 10  $\mu\text{M}$ .<sup>34</sup> Thus, the fact that both slopes were close to unity should be evidence for a unimolecular channel process.<sup>32b</sup> Given the lipophilicity and flexibility of the appended Phe tripeptide chains, we propose that the rigid aromatic backbone of the inserted channel molecules was oriented in the middle of the bilayers and the peptide chains were forced by surrounding lipid molecules to stand up and down (Figure 7b). The peptide chains on both sides were pushed by the lipid molecules to shrink, but the molecule as a whole still formed a channel across the bilayer to mediate the transport of the ions. For 4 and 5, the  $n$  values could not be determined accurately because their lower  $V_0$  values did not allow a similar linear relationship to be established. However, since they possess even longer helical backbones, it is reasonable to propose that they also transport the ions in a unimolecular state.

In conclusion, we have demonstrated that hydrogen-bonded aromatic hydrazide foldamers can mediate the transmembrane transport of cations by forming a helical tube across lipid bilayers. The two longest oligomeric and polymeric foldamers exhibited  $\text{NH}_4^+/\text{K}^+$  selectivities higher than that of natural gramicidin A, while the transport of a short pentameric foldamer for  $\text{Tl}^+$  achieved an efficiency close to that of gramicidin A. The results illustrate that artificial channels can reach high transport selectivities and efficiencies by careful control of their conformation. The establishment of the cation dehydration mechanism also suggests that we may design new helical systems in the future for transporting a cation in a more specific way by

introducing ionic groups (e.g., carboxylate) to tune the dehydration and to reach pH-controlled transport.

## ■ ASSOCIATED CONTENT

### ● Supporting Information

Synthetic procedures and characterization data for 1–5 and detailed procedures and results for H<sup>+</sup> transport, patch clamp, stopped-flow, ECD, and <sup>1</sup>H NMR binding experiments. This material is available free of charge via the Internet at <http://pubs.acs.org>.

## ■ AUTHOR INFORMATION

### Corresponding Authors

houjl@fudan.edu.cn

ztli@fudan.edu.cn

### Notes

The authors declare no competing financial interest.

## ■ ACKNOWLEDGMENTS

This work was supported by the Ministry of Science and Technology of China (2013CB834501), the Ministry of Education of China (IRT1117), STCSM (13NM1400200), and the Open Project of the State Key Laboratory of Supramolecular Structure and Materials (sklssm201434).

## ■ REFERENCES

- (1) Hille, B. *Ionic Channels of Excitable Membranes*, 3rd ed.; Sinauer Associates: Sunderland, MA, 2001.
- (2) Andersen, O. S.; Koeppel, R. E., II; Roux, B. In *Biological Membrane Ion Channels*; Chung, S.-H., Andersen, O. S., Krishnamurthy, V., Eds.; Springer: New York, 2007; Chapter 2.
- (3) Kelkar, D. A.; Chattopadhyay, A. *Biochim. Biophys. Acta* **2007**, *1768*, 2011.
- (4) Matile, S.; Fyles, T. *Acc. Chem. Res.* **2013**, *46*, 2741.
- (5) Sakai, N.; Mareda, J.; Matile, S. *Acc. Chem. Res.* **2005**, *38*, 79.
- (6) (a) Gong, B.; Shao, Z. *Acc. Chem. Res.* **2013**, *46*, 2856. (b) Montenegro, J.; Ghadiri, M. R.; Granja, J. R. *Acc. Chem. Res.* **2013**, *46*, 2955.
- (7) (a) Kaucher, M. S.; Harrell, W. A.; Davis, J. T. *J. Am. Chem. Soc.* **2006**, *128*, 38. (b) Li, X.; Wu, Y.-D.; Yang, D. *Acc. Chem. Res.* **2008**, *41*, 1428.
- (8) (a) Gokel, G. W.; Murillo, O. *Acc. Chem. Res.* **1996**, *29*, 425. (b) Hu, X.-B.; Chen, Z.; Tang, G.; Hou, J.-L.; Li, Z.-T. *J. Am. Chem. Soc.* **2012**, *134*, 8384.
- (9) Akerfeldt, K. S.; Lear, J. D.; Wasserman, Z. R.; Chung, L. A.; DeGrado, W. F. *Acc. Chem. Res.* **1993**, *26*, 191.
- (10) (a) Schrey, A.; Vescovi, A.; Knoll, A.; Rikert, C.; Koert, U. *Angew. Chem., Int. Ed.* **2000**, *39*, 900. (b) Mayer, M.; Yang, J. *Acc. Chem. Res.* **2013**, *46*, 2998.
- (11) (a) Muraoka, T.; Shima, T.; Hamada, T.; Morita, M.; Takagi, M.; Tabata, K. V.; Noji, H.; Kinbara, K. *J. Am. Chem. Soc.* **2012**, *134*, 19788. (b) Zhao, Y.; Cho, H.; Widanapathirana, L.; Zhang, S. *Acc. Chem. Res.* **2013**, *46*, 2763.
- (12) (a) Tanaka, Y.; Kobuke, Y.; Sokabe, M. *Angew. Chem., Int. Ed. Engl.* **1995**, *34*, 693. (b) Tedesco, M. M.; Ghebremariam, B.; Sakai, N.; Matile, S. *Angew. Chem., Int. Ed.* **1999**, *38*, 540. (c) Sakai, N.; Kamikawa, Y.; Nishii, M.; Matsuoka, T.; Kato, T.; Matile, S. *J. Am. Chem. Soc.* **2006**, *128*, 2218. (d) Jung, M.; Kim, H.; Baek, K.; Kim, K. *Angew. Chem., Int. Ed.* **2008**, *47*, 5755.
- (13) (a) Smith, E. M.; Holmes, D. L.; Shaka, A. J.; Nowick, J. S. *J. Org. Chem.* **1997**, *62*, 7906. (b) Huc, I. *Eur. J. Org. Chem.* **2004**, *17*. (c) Gong, B. *Acc. Chem. Res.* **2008**, *41*, 1376. (d) Zhang, D.-W.; Zhao, Z.; Hou, J.-L.; Li, Z.-T. *Chem. Rev.* **2012**, *112*, 5271.
- (14) Hou, J.-L.; Shao, X.-B.; Chen, G.-J.; Zhou, Y.-X.; Jiang, X.-K.; Li, Z.-T. *J. Am. Chem. Soc.* **2004**, *126*, 12386.
- (15) Chen, L.; Si, W.; Zhang, L.; Tang, G.; Li, Z.-T.; Hou, J.-L. *J. Am. Chem. Soc.* **2013**, *135*, 2152.
- (16) Holding, S. R.; Meehan, E. *Molecular Weight Characterization of Synthetic Polymers*; Rapra Technology: Shrewsbury, U.K., 1995.
- (17) Jeon, Y. J.; Kim, H.; Jon, S.; Selvapalam, N.; Oh, D. Y.; Seo, I.; Park, C.-S.; Jung, S. R.; Koh, D.-S.; Kim, K. *J. Am. Chem. Soc.* **2004**, *126*, 15944.
- (18) The molar concentration of polymer 5 was calculated directly using the molecular weight determined from the standard curve method.
- (19) Busschaert, N.; Wenzel, M.; Light, M. E.; Iglesias-Hernandez, P.; Perez-Tomas, R.; Gale, P. A. *J. Am. Chem. Soc.* **2011**, *133*, 14136.
- (20) Gale, P. A.; Tong, C. C.; Haynes, C. J. E.; Adeosun, O.; Gross, D. E.; Karnas, E.; Sedenberg, E. M.; Quesada, R.; Sessler, J. L. *J. Am. Chem. Soc.* **2010**, *132*, 3240.
- (21) McNally, B. A.; O'Neil, E. J.; Nguyen, A.; Smith, B. D. *J. Am. Chem. Soc.* **2008**, *130*, 17274.
- (22) Matile, S.; Sakai, N.; Hennig, A. Transport Experiments in Membranes. In *Supramolecular Chemistry: From Molecules to Nanomaterials*; Steed, J. W., Gale, P. A., Eds.; Wiley: New York, 2012.
- (23) Ashley, R. H. *Ion Channels: A Practical Approach*; Oxford University Press, Oxford, U.K., 1995.
- (24) Chui, J. K. W.; Fyles, T. M. *Chem. Soc. Rev.* **2012**, *41*, 148.
- (25) The current of polymer 5 at a given clamp voltage is the average current of all observed conductance states.
- (26) Andersen, O. S. *Biophys. J.* **1983**, *41*, 119.
- (27) Fyles, T. M.; Looock, D.; van Straaten-Nijenhuis, W. F.; Zhou, X. J. *Org. Chem.* **1996**, *61*, 8866.
- (28) Eisenman, G.; Horn, R. J. *Membr. Biol.* **1983**, *76*, 197.
- (29) Neher, E.; Sandblom, J.; Eisenman, G. *J. Membr. Biol.* **1978**, *40*, 97.
- (30) Xu, X.-N.; Wang, L.; Wang, G.-T.; Lin, J.-B.; Li, G.-Y.; Jiang, X.-K.; Li, Z.-T. *Chem.—Eur. J.* **2009**, *15*, 5763.
- (31) Urban, B. W.; Hladky, S. B.; Haydon, D. A. *Biochim. Biophys. Acta* **1980**, *602*, 331.
- (32) (a) Moore, H.-P.; Raftery, M. A. *Proc. Natl. Acad. Sci. U.S.A.* **1980**, *77*, 4509. (b) Bruggemann, E. P.; Kayalar, C. *Proc. Natl. Acad. Sci. U.S.A.* **1986**, *83*, 4273.
- (33) Pauling, L. *Nature of the Chemical Bond and Structure of Molecules and Crystals*, 3rd Ed.; Cornell University Press: Ithaca, NY, 1960.
- (34) Bhosale, S.; Matile, S. *Chirality* **2006**, *18*, 849.